NOTES AND CORRESPONDENCE

The Impact of Satellite-Derived Atmospheric Motion Vectors on Mesoscale Forecasts over Hawaii*

T. CHERUBINI AND S. BUSINGER

Department of Meteorology, University of Hawaii at Manoa, Honolulu, Hawaii

C. VELDEN

CIMSS, University of Wisconsin—Madison, Madison, Wisconsin

R. OGASAWARA

Subaru Observatory, Hilo, Hawaii

(Manuscript received 13 July 2005, in final form 19 September 2005)

ABSTRACT

Tropospheric motions can be inferred from geostationary satellites by tracking clouds and water vapor in sequential imagery. These atmospheric motion vectors (AMV) have been operationally assimilated into global models for the past three decades, with positive forecast impacts. This paper presents results from a study to assess the impact of AMV derived from Geostationary Operational Environmental Satellite (GOES) imagery on *mesoscale* forecasts over the conventional data-poor central North Pacific region. These AMV are derived using the latest automated processing methodologies by the University of Wisconsin—Cooperative Institute for Meteorological Satellite Studies (CIMSS). For a test case, a poorly forecast subtropical cyclone (kona low) that occurred over Hawaii on 23–27 February 1997 was chosen. The Local Analysis and Prediction System (LAPS) was used to assimilate *GOES-9* AMV data and to produce fifth-generation Pennsylvania State University–NCAR Mesoscale Model (MM5) initial conditions. The satellite wind assimilation is carried out on the 27-km-resolution domain covering the central Pacific area. The MM5 was run with three two-way nested domains (27, 9, and 3 km), with the innermost domain moving with the kona low. The AMV data are found to influence the cyclone's development, improving the prediction of the cyclone's central pressure and the track of the low's center. Since September 2003, *GOES-10* AMV data have been routinely accessed from CIMSS in real time and assimilated into the University of Hawaii (UH) LAPS, providing high-resolution initial conditions for twice-daily runs of MM5 at the Mauna Kea Weather Center collocated at the UH. It is found that the direct assimilation of AMV data into LAPS has a positive impact on the forecast accuracy of the UH LAPS/MM5 operational forecasting system when validated with observations in Hawaii. The implications of the results are discussed.

1. Introduction

A lack of observational data over the surrounding ocean makes weather forecasting a special challenge in Hawaii. The central North Pacific region that encompasses the Hawaiian Islands is characterized by rapidly evolving mesoscale systems, which compound the forecast challenge. Forecast errors can frequently be traced to errors in initial conditions, particularly in dynamically active areas where observational data are scarce (Klinker et al. 1998). Temperature and, to some extent, moisture fields from polar-orbiting satellite sensors are currently assimilated in global analyses, providing a good source of information where conventional data are sparse. However, by comparison, it is less clear if atmospheric motion vectors (AMV) are optimally as-

* SOEST Contribution Number 6767.

Corresponding author address: Dr. Tiziana Cherubini, 2525 Correa Rd., HIG 367, Honolulu, HI 96822.
E-mail: tiziana@hawaii.edu

similated by the global models, especially with regard to retaining mesoscale information.

This study investigates the impact of the assimilation of satellite-derived wind data on the accuracy of *mesoscale* model forecasts over the data-sparse central Pacific Ocean. The focus of this paper is primarily on the impact of assimilating AMV data into the fifth-generation Pennsylvania State University–National Center for Atmospheric Research (PSU–NCAR) Mesoscale Model (MM5) initial conditions. However, results from the addition of radiance data are also included in the study. The investigation begins with a case study analysis of a poorly forecast subtropical cyclone (kona low) that occurred over Hawaii during 23–27 February 1997. Morrison and Businger (2001) documented the storm's evolution and impact using all available operational and observational data (including all ship and buoy reports). Their subjective analyses also had the benefit of data from the National Centers for Environmental Prediction (NCEP)–NCAR reanalysis project. *Geostationary Operational Environmental Satellite-9* (*GOES-9*) AMV data and *GOES-9* radiances from three channels, visible (VIS), infrared (IR), and water vapor (WV), were obtained from University of Wisconsin—Cooperative Institute for Meteorological Satellite Studies (CIMSS) for the period of investigation. The second part of the study focuses on an extended period of continuous AMV assimilation. *GOES-10* AMV data have been operationally ingested into the University of Hawaii Local Analysis and Prediction System (LAPS) to produce local high-resolution meteorological analyses since September 2003 at the Mauna Kea Weather Center (MKWC; http://mkwc.ifa.hawaii.edu). These analyses, in turn, are used as initial conditions for the operational version of MM5 run at the MKWC, which is a weather research and forecast facility that provides support to the Mauna Kea observatories in the form of custom weather observations and forecasts (Businger et al. 2002). The MM5 has been run operationally at MKWC since January 1999.

2. AMV dataset description

The derivation of AMV at national data processing centers has evolved considerably since the original conception in the early 1970s. CIMSS, a National Oceanic and Atmospheric Administration/National Environmental Satellite, Data, and Information Service (NOAA/NESDIS) cooperative institute, has played a prominent role in the advancement of automated AMV processing procedures, leading to positive impacts on weather analysis and forecasting applications (Neiman et al. 1997; Velden et al. 1997, 2005). Current automated procedures provide estimates of wind at multiple levels using ordered sequences of multispectral satellite images. The algorithms derive wind observations from the VIS, IR window, and WV absorption bands. Extraction of AMV from the WV band provides wind data in the regions devoid of cloud in the middle–upper troposphere (Velden et al. 1997).

AMV data are typically distributed in the vertical over the entire troposphere, but exhibit a bimodal profile with a concentration of vectors in the lower troposphere between 900 and 800 mb, and a second maximum between 200 and 300 mb (Fig. 1a). The AMV wind data are not uniformly distributed in the horizontal; rather the distribution reflects the locations of clouds and water vapor gradients (Figs. 1b–d).

3. Data assimilation and model setup

The LAPS (McGinley 1989; McGinley et al. 1991) has been adapted at the MKWC to assimilate AMV data and other operational and satellite data to produce local high-resolution analyses over the central North Pacific Ocean. The LAPS was developed at the NOAA's Forecast System Laboratory to merge all the available data sources over the area of interest and produce coherent analyses of the atmosphere. The LAPS first performs an analysis of the surface fields, followed by a wind analysis, a temperature analysis, and finally a cloud-field analysis. All of the above make use of a first-guess field, usually provided by a global numerical weather prediction model. The LAPS wind analysis uses all available data sources in a two-pass objective analysis. Background model grids are used as a first-guess analysis from which observation residuals are calculated. The observation residuals are subject to quality control (QC) checks. AMV data are rejected when the difference between the AMV value and the background model grid is greater than 10 m s^{-1}. The observation residuals are spread vertically onto grid points within 50 hPa of the observation's level by means of an exponential weighting term and horizontally using a Barnes exponential weighting function with a radius of influence that is a spatially varying function of the data density. More details about LAPS wind analysis can be found in Albers (1995). For the case under investigation about 6% of the AMV data were rejected by the QC check. An average of 4% to 8% of the AMV data gathered at MKWC are rejected by the QC check in the operational analysis process. Inspection of the rejected wind data does not reveal a coherent signal; rather the

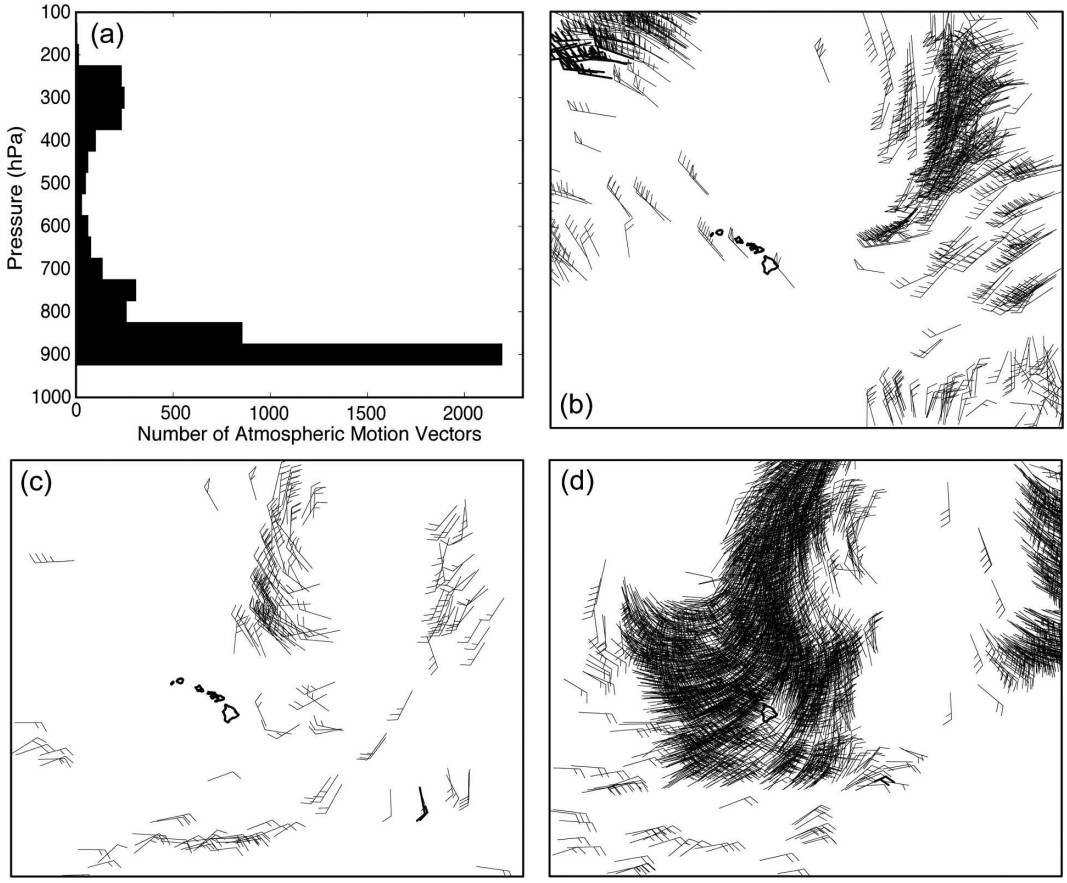

FIG. 1. (a) AMV data distribution with pressure at 1800 UTC 23 Feb 1997. Data are binned every 50 mb. Also shown are AMV data for 1800 UTC 23 Feb 1997 plotted at (b) 300, (c) 600, and (d) 900 mb.

rejected data are uncorrelated. Therefore, it is safe to assume that most of the smaller-scale AMV information signal is not lost through the QC process (perhaps not a valid assumption for global model AMV assimilation).

The mesoscale numerical model used at the MKWC, and in this study, is the MM5 (Grell et al. 1995). The MM5 is a nonhydrostatic primitive equation model with a terrain-following coordinate. It has multiple nesting capabilities to enhance the simulation over the area of interest. A configuration of three two-way nested domains was chosen for the case study presented in this paper (Fig. 2). The horizontal resolution is 27 km for the outermost domain covering the central Pacific area, 9 km for the nested domain, and 3 km for the innermost domain, which moves along with the kona low. Thirty-three sigma levels, denser in the lower troposphere, are used, with the top level at 100 mb. The MM5 physics package uses the grid-resolvable Reisner-2 moisture scheme (Reisner et al. 1998) that includes graupel and ice condensation nuclei and allows coexistence of mixed water phases; the Kain–Fritsch cumulus convection scheme (Kain and Fritsch 1990); a high-resolution Medium-Range Forecast model boundary layer scheme (Throen and Mahrt 1986); and a longwave/shortwave radiation scheme that allows interaction with water vapor, clouds, precipitation, and the surface (Stephens 1978; Garand 1983). For our operational runs, MM5 boundary conditions are updated every 6 h using the Global Forecasting System (GFS) model output.

To produce the best simulation possible for the case study under investigation, the sensitivity experiments described in this section are carried out in "archived mode" in which general circulation model analyses (not the forecasts) provide boundary conditions. The European Centre for Medium-Range Weather Forecasts (ECMWF) 40-yr Re-Analysis data (hereafter referred to as ERA-40) are used for the case under investigation. The ERA-40 analyses have spectral resolution T159, corresponding to ~125 km horizontal resolution in the Tropics, and are available on 60 vertical levels. It should be noted that operationally produced GOES AMV by NOAA/NESDIS are included in the input datastream for the ERA-40 analyses.

Four sensitivity experiments are carried out with

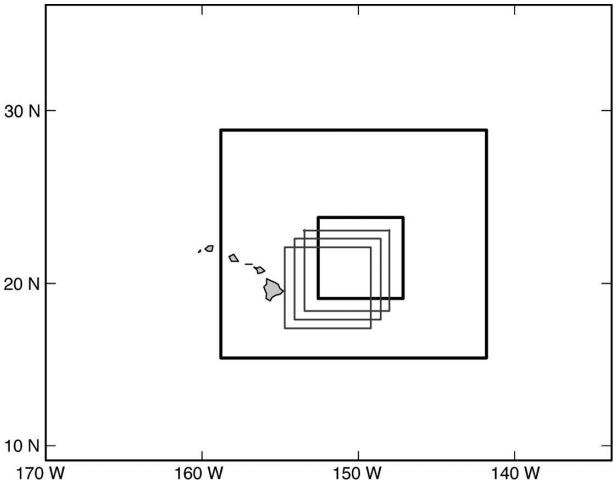

FIG. 2. MM5 outer, middle, and inner domains, with 27-, 9-, and 3-km grid resolution, respectively. The innermost domain is allowed to move along with the kona low system (gray squares).

MM5, using four different sets of MM5 boundary and initial conditions:

- Experiment 1—MM5 initial and boundary conditions are created using ERA-40 valid at 1800 UTC 23 February 1997. Only the outermost domain with 27-km grid spacing is used in this experiment.
- Experiment 2—*GOES-9* AMV data for 1800 UTC 23 February 1997 are assimilated through LAPS into MM5 initial conditions. The MM5 boundary conditions are updated using ERA-40 only.
- Experiment 3—*GOES-9* AMV data are assimilated through LAPS into MM5 initial and boundary conditions throughout the model run. A LAPS analysis is created every 6 h and is used to provide the initial and boundary conditions. No nudging is performed.
- Experiment 4—*GOES-9* AMV and radiance data for 1800 UTC 23 February 1997 are assimilated through LAPS into MM5 initial conditions. The MM5 boundary conditions are updated using ERA-40 only.

Experiment 1 employs a relatively coarse model resolution and the results may be considered characteristic of global model runs. Experiments 2 and 3 are designed in particular to investigate the impact of local assimilation of AMV on the simulation. Experiment 4 is included as the configuration closest to the one run operationally at the MKWC. Thus, the results of this experiment are germane to the operational results presented in section 5.

To investigate the model's sensitivity to resolution and to determine to what degree the differences in the results of experiments 1 and 2 were due to differences in domain configuration, two additional experiments were conducted (not shown). Both were run without AMV assimilation, and utilized two and three nested-domain configurations, respectively. Results from these resolution experiments support the conclusion that the differences between experiments 1 and 2 are primarily because of the assimilation of the AMV data.

In the next section the simulated cyclone development in the four experiments will be compared. The storm's central pressure and the track of the low center were calculated using the 3-km grid domain whenever possible. Early in the simulations, the 9- or 27-km domains were used, because the innermost domain did not cover the area of the incipient system. Two-way nesting guarantees consistency between different grids.

4. Results of case-study sensitivity experiments

Morrison and Businger (2001) document the role of vorticity advection and divergence aloft in kona low initiation. The results of the numerical experiments should be sensitive to differences in the flow fields aloft associated with the assimilation of *GOES-9* AMV and radiance data in the initial analyses. The vector-difference wind field between experiments 1 and 2 shows an anticyclonic anomaly on the south side of the trough at the surface and a cyclonic anomaly in the difference field east of Hawaii (Fig. 3a). At 900 mb the greatest vector differences are seen southwest of the surface low, where northeasterly flow is underestimated in the absence of AMV (Fig. 3b). Enhanced vector differences are also seen near the center of the surface high and in the area east of the surface trough.

Divergence fields derived from the initial analyses for experiments 1 and 2 exhibit noticeable differences in both the lower and upper atmosphere (Fig. 4). Figure 4a shows positive divergence aloft located in the vicinity of the surface trough. Divergence residuals show mixed values surrounding the trough, but in general the area of divergence aloft is reduced over the surface trough when AMV data are included in the analysis. In the lower atmosphere (900 mb), the area of convergence is reduced slightly when AMV data are included in the analysis (Figs. 4c and 4d).

These somewhat subtle differences in the analyzed wind field contribute to greater deepening of the forecast storm system in the MM5 simulations (Fig. 5). The MM5 is able to capture the deepening trend of the kona low significantly better than the NCEP Aviation Model (AVN) forecasts, but the predicted values are not as low as estimated from subjective analysis. The underestimation of the lowest central pressure by the simu-

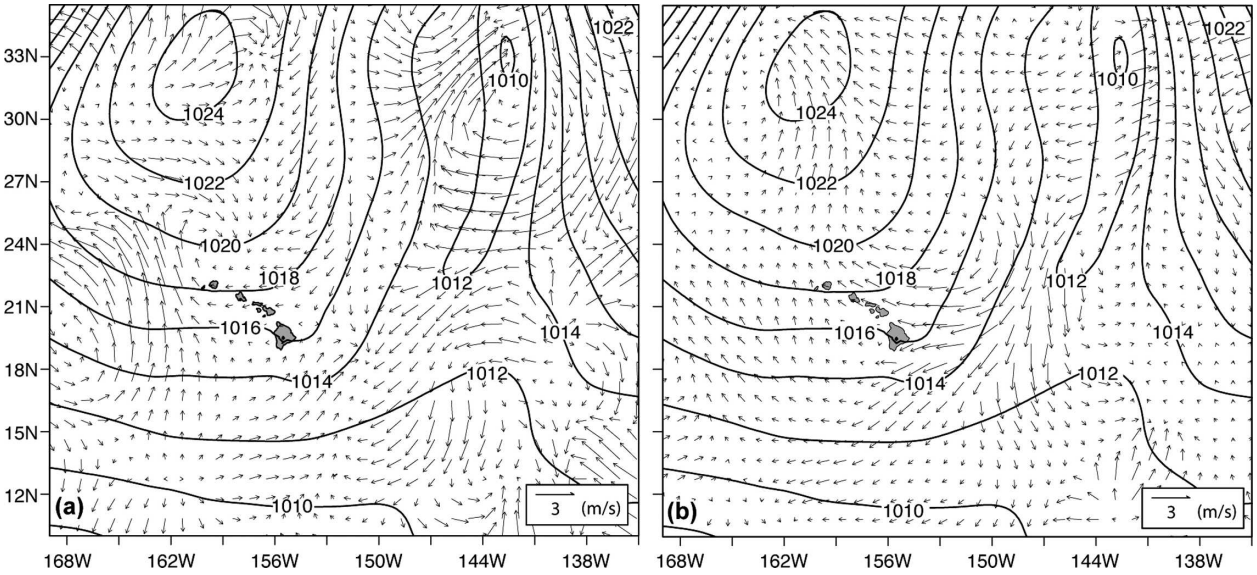

FIG. 3. Vector difference at (a) 300 and (b) 900 mb between experiment 2 initial conditions and experiment 1 initial conditions at 1800 UTC 23 Feb 1997. Mean sea level pressure (solid contours) is overlaid for reference.

lations may be due in part to the fact that the central pressure of the initial disturbance was underestimated by the initial analysis (cf. dashed and solid black lines in Fig. 5). Since the MM5 boundary conditions were from archived ECMWF analyses, the reader is cautioned that a direct comparison between MM5 forecasts and the AVN model forecast is not entirely appropriate. Nevertheless, the AVN is shown as reference of what was available at the time of the storm.

In the absence of AMV data (experiment 1), the simulated storm system begins to weaken prior to the storm's analyzed *mature stage*, the time of lowest sea level pressure in the subjective analysis (Figs. 5a and 6a). When the assimilation of AMV data takes place at the initial time only (experiment 2), the impact of assimilated winds is greatest during the first 6 h of simulation, and the positive impact tends to diminish as the simulation progresses. The low continues to deepen after the mature stage, rather than fill as was observed. This may reflect orographic impacts as the surface low nears Hawaii.

It is significant that when AMV data are included in the boundary conditions throughout the simulation (experiment 3) the result is a deeper storm, which begins to fill in the last ~12 h of the simulation as was observed (Figs. 5b and 6b). The best simulation of the storm's central pressure during the first 30 h of simulation results when radiances and AMV data are assimilated in the model initial conditions (experiment 4). A better analysis of the moisture distribution provided by LAPS results in a faster deepening rate, confirming the importance of latent heating in addition to dry dynamics for an accurate simulation. However, a weakening trend during the mature stage in this experiment may reflect the lack of data assimilation after the initial time.

Turning to the track forecasts, MM5 tends to propagate the kona low system too fast during the *intensifying stage* (period of most rapid deepening in the subjective analysis in Fig. 5) in experiment 1 (Fig. 7a). The inclusion of AMV data in the model initial conditions (experiment 2) slows the system propagation during the intensifying stage, resulting in better agreement between observed and modeled storm tracks during the first ~30 h of simulation (Fig. 7a). Experiments 1, 2, and 4 all show excursions in the storm track as the kona low approaches Hawaii during the latter part of the simulations; these excursions were not reflected in the subjective analysis. When the model fields are examined in detail, it is apparent that orographic influences and enhanced model resolution account for these excursions (not shown). Of the four simulations, the tracks in experiments 3 and 4 are closest to the observed track (Fig. 7b). Experiment 3 exhibits the smoothest track and is closest to the observed track at the end of the simulation (Fig. 7b), suggesting the benefit of the assimilation of AMV data throughout the simulation.

The ability of the simulations to reproduce the mesoscale structures of the kona low is generally beyond the scope of this paper. However, some observations can be made from analyses of the MM5 output (e.g., Fig. 6). When the region of coldest cloud-top tempera-

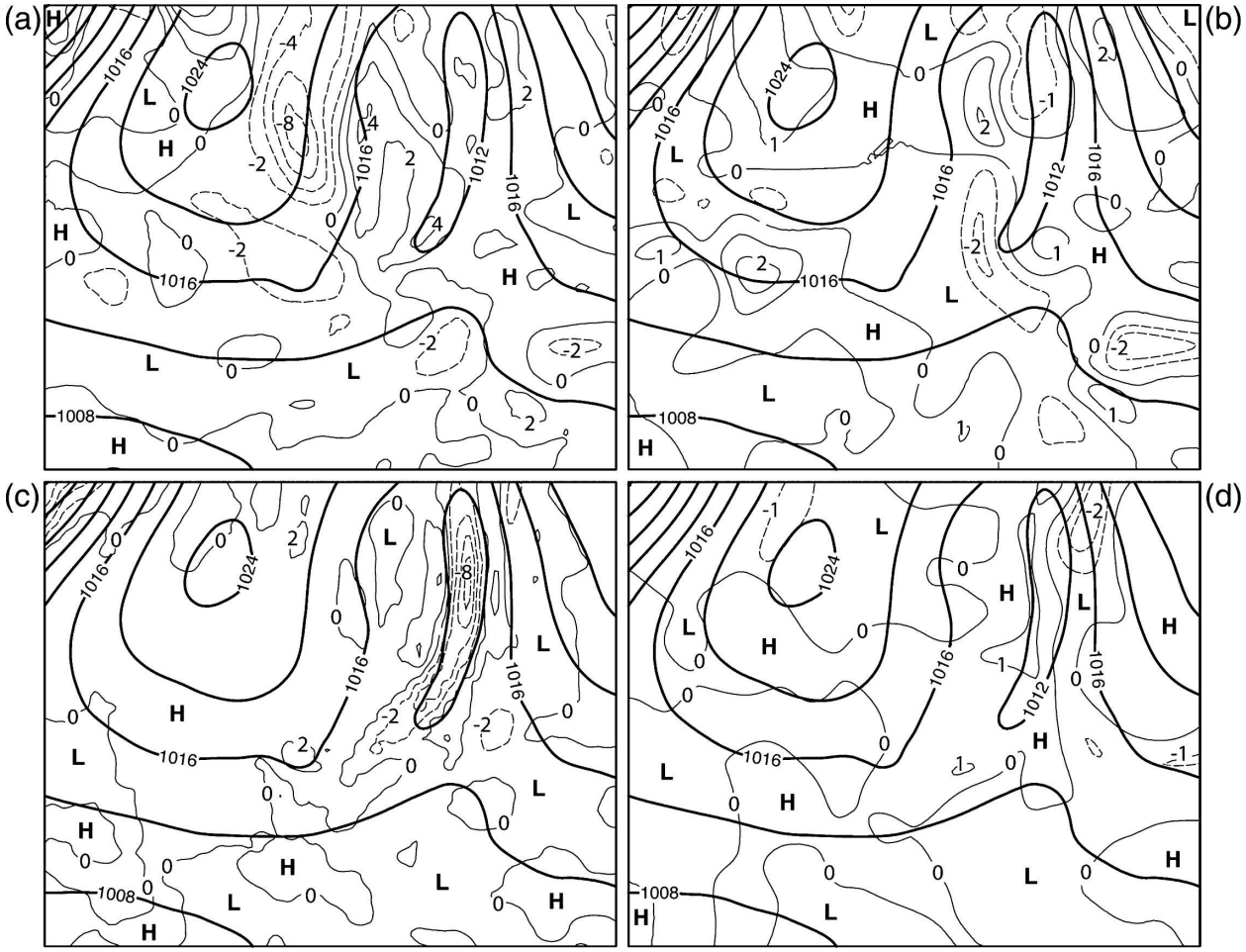

FIG. 4. (a) Initial analysis of 300-mb divergence (thin lines) for experiment 2, (b) 300-mb divergence residual (experiment 2 divergence − experiment 1 divergence), (c) initial analysis of 900-mb divergence (thin lines) for experiment 2, and (d) 900-mb divergence residual. Thick lines in (a)–(d) show the analysis of sea level pressure at 1800 UTC 23 Feb 1997.

tures in the satellite imagery (Fig. 6c) is compared with the precipitable water forecast for the mature stage in the kona low in experiment 3 (Fig. 6d), a coincidence of features is apparent. Patterns of convection in cold upper-level lows have previously been linked to enhanced vorticity in the upper troposphere (Businger and Reed 1989). The suggestion is that the direct assimilation of AMV throughout the LAPS/MM5 run results in a predicted vorticity field aloft with mesoscale features that mirror those observed during the mature stage of the storm.

5. Impact of GOES AMV and radiance data on operational MKWC forecasts

GOES-10 AMV data have been obtained from CIMSS at MKWC and operationally assimilated into LAPS since September 2003. In addition to the AMV data, LAPS operationally assimilates all available synoptic and maritime data, two soundings, and radiances from three *GOES-10* channels (IR, VIS, and VW). Analyses verifying at 0000, 0600, 1200, and 1800 UTC are produced daily and used to initialize two daily MM5 runs (0000 and 1200 UTC). These MM5 forecasts with full LAPS input are run in parallel with two MM5 runs without LAPS input. NCEP GFS analyses and forecasts serve as the initial and boundary conditions for these comparison runs. Finite computational resources preclude a third set of operational runs initialized only with AMV data. Therefore, the results in this section compare MM5 forecasts run with and without the full LAPS data assimilation in the initial conditions.

The number of *GOES-10* AMV data ingested into LAPS varies from day to day depending on environmental conditions (Fig. 8). The two distributions shown in Fig. 8 differ because the *GOES-10* visible channel is

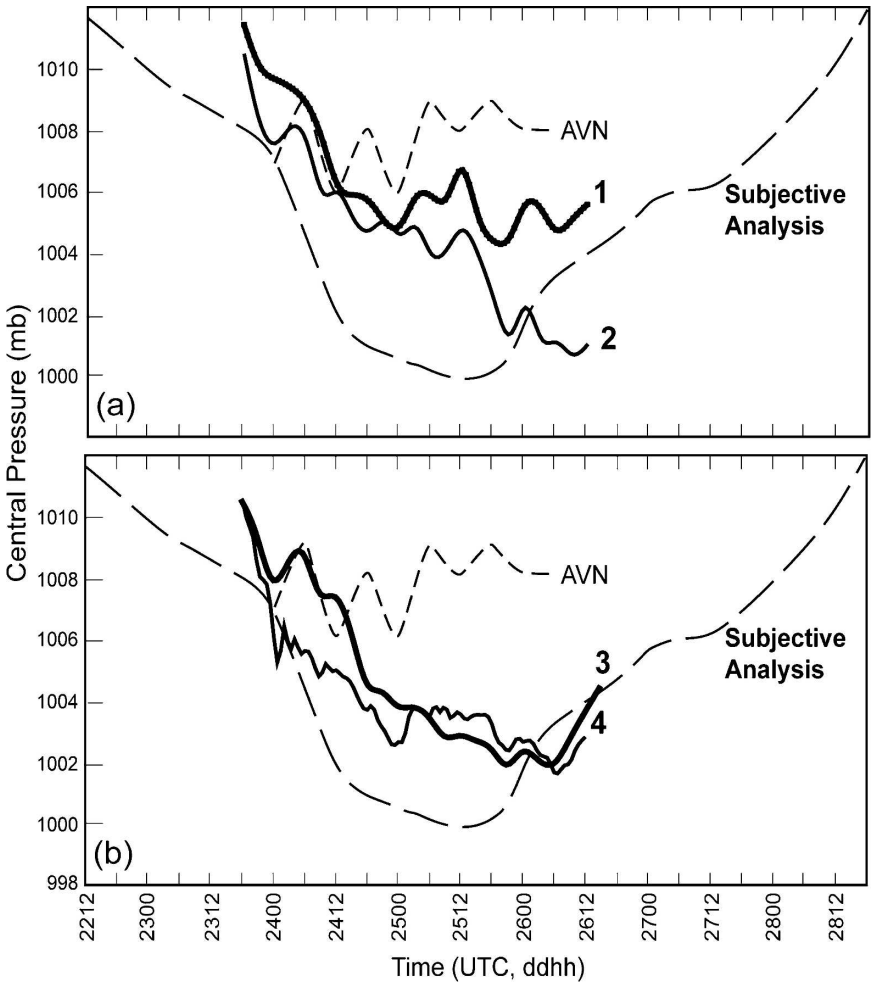

FIG. 5. Time series of kona low central sea level pressure. (a) The heavy solid line shows the MM5 experiment 1 simulation, and the thin solid line shows the experiment 2 simulation. (b) The heavy solid line shows the experiment 3 simulation, and the thin solid line shows the experiment 4 simulation. The subjective analysis from Morrison and Businger (2001) (long dashes) and NCEP AVN simulation (short dashes) are also shown.

not available at 1200 UTC. Although AMV are distributed throughout the troposphere, they show a bimodal distribution. The 850-mb peak is associated with the tracking of low-level clouds. The 250-mb peak comes from tracking clouds in both the WV and infrared channels. Given the high number of AMV data available, compared with any other wind data available in LAPS (synoptic stations and two soundings) they have a higher weight in the analysis. *GOES-10* radiances contribute primarily to the moisture field in the analyses.

The verification period covers February and March 2004. The verification procedure is based on the calculation of root-mean-square errors (RMSE) for select MM5 fields at increasing forecast times. The RMSE is calculated comparing mean sea level pressure, temperature, relative humidity, and wind components at 850 mb with the LAPS NCEP GFS analyses verifying at the forecast time (see Fig. 9). Data used in the verification process cover the model domain that extends from 5° to 35°N and from 140° to 170°W. This verification approach is a model grid point to analysis grid point as opposed to a model grid point to observation location verification approach. Given the paucity of synoptic observations in the central Pacific area, the first approach is preferred since it provides larger samples on which to run the statistical analyses (Cherubini et al. 2002). The ideal verification procedure encompasses both methodologies. A drop in the RMSE is evident on the first 24 h of simulation, when LAPS is used in the model initial conditions (Fig. 9).

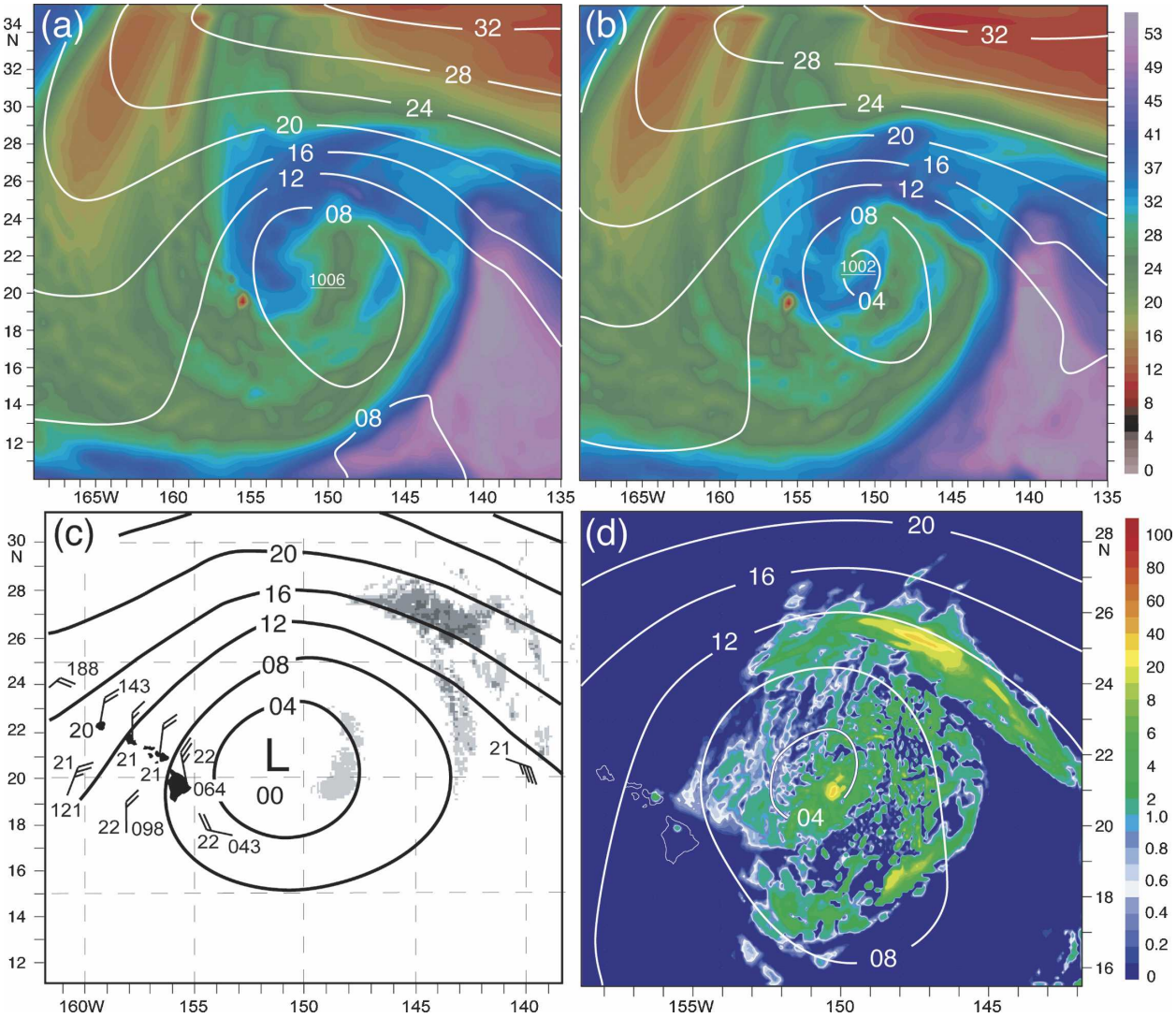

FIG. 6. Sea level pressure (every 4 mb) for the mature stage of the kona low at 1200 UTC 25 Feb 1997. (a) Outer domain output for experiment 1 showing 24-h forecast of precipitable water (color shading; mm). (b) Outer domain output for experiment 3 showing 24-h forecast of precipitable water (color shading; mm). (c) Subjective surface analysis, with IR temperature <-40°C from *GOES-9* (after Morrison and Businger 2001). (d) Middle domain output for experiment 3 showing 24-h forecast of 3-h accumulated rainfall (color shading; mm).

Since the data assimilation is performed at the initial time only, the impact of assimilated observations is greatest during the first 24 h of the simulation. The positive impact diminishes as the simulation progresses and the MM5 boundary conditions are updated. As a result, the model simulation in time converges to the simulation without assimilation. The reduction in error is larger for the 0000 UTC forecast cycle than for the 1200 UTC cycle. This difference may be due to the lack of visible channel data at 1200 UTC over the central Pacific, which impacts both radiance and AMV data.

In the following discussion, we will focus on the t_0 + 12 h verification time only. Output from forecasts with a starting time of 0000 UTC (t_0) is evaluated, to focus on the time when the impact of the LAPS data assimilation may be greatest. The RMSE for the MM5 12-h forecasts initialized with LAPS (solid line) are consistently smaller than the RMSE for MM5 forecasts initialized without LAPS (thin dashed line) for most of the fields analyzed (Fig. 10). The largest impact is seen in the sea level pressure and relative humidity fields, with good impact on wind fields as well. The temperature field shows less impact from data assimilation, perhaps a reflection of better temperature analyses in the GFS

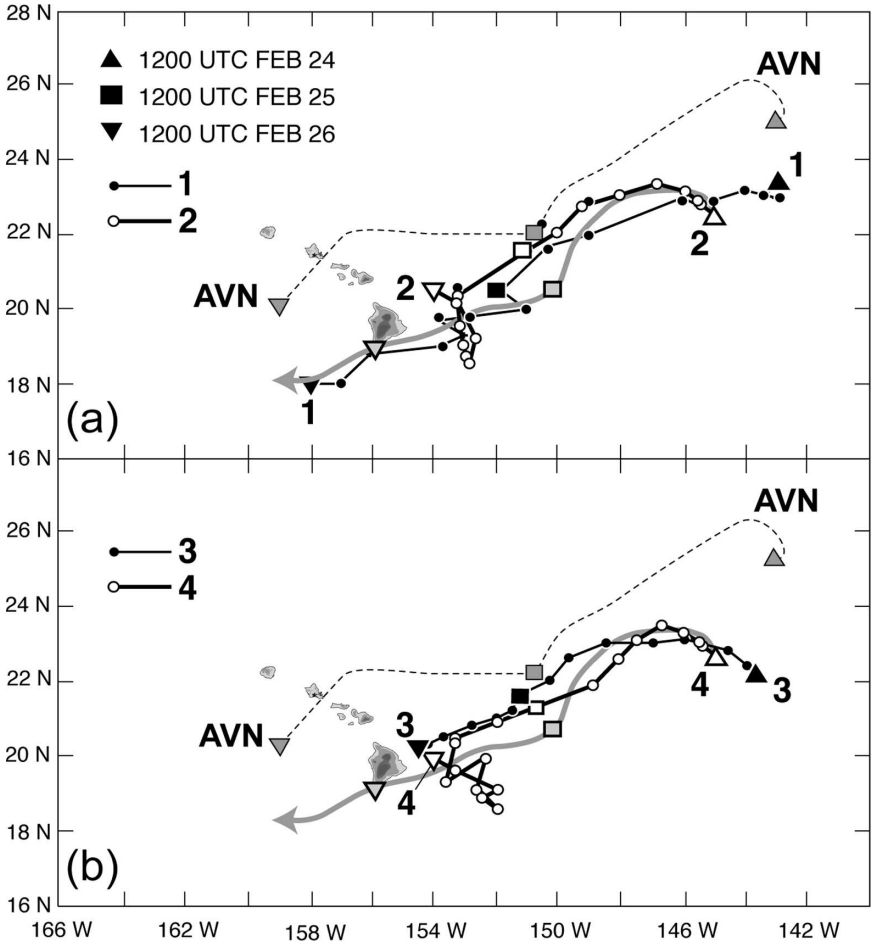

FIG. 7. Forecast storm tracks associated with the four sensitivity experiments are shown along with the subjective analysis (thick gray line; after Morrison and Businger 2001) and the forecast track from the global model simulation (thin dashed line). (a) The labeled lines show the forecast storm tracks from experiments 1 and 2. (b) The labeled lines show the forecast storm tracks from experiments 3 and 4.

(from improved methods of radiance assimilation). For forecasts with a 1200 UTC starting time the impact of using LAPS on RMSE is smaller than was found for the 0000 cycle, but it was still positive (not shown).

6. Conclusions and discussion

The AMV data represent an important resource for improving the analysis of the atmospheric flow over data-sparse regions, particularly over open oceans. In this paper, we show that application of a simple procedure to assimilate AMV data directly into MM5 initial conditions has a verifiable positive impact on the simulation accuracy. While AMV are assimilated into global models, the retention of information on smaller scales may be lost by the quality control and inherent smoothing of the observations in the coarser-resolution initial analyses.

A poorly forecast subtropical cyclone was chosen for a series of sensitivity experiments. Simulations with and without assimilation of *GOES-9* AMV data in the model's initial condition were conducted. The results show that the added information on the model flow provided by AMV data contributes to a reduction in the system's track error. Moreover, a better agreement is found between the subjectively analyzed and model surface fields when the AMV contribute to the boundary conditions throughout the model run.

A more accurate knowledge of the moisture distribution through assimilation of radiances from *GOES-9* IR, WV, and VIS channels in the model initial conditions contributes to model accuracy as well. Given the correlation between dynamic and thermodynamic pro-

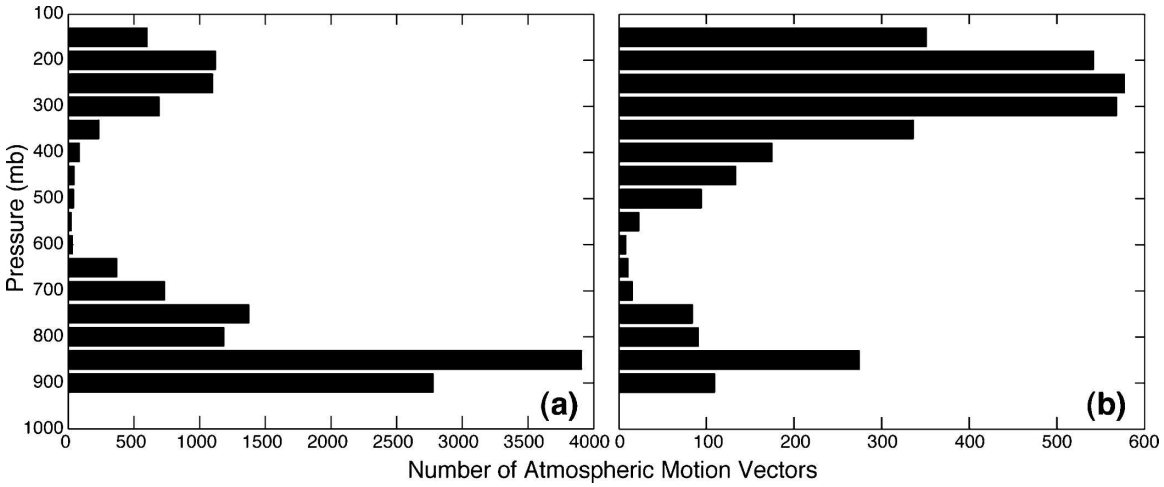

FIG. 8. Average counts of AMV data that pass LAPS quality control binned every 50 mb: (a) 0000 and (b) 1200 UTC.

cesses, the synergy of assimilated wind and radiance data provides the best prediction.

Since September 2003, *GOES-10* AMV data are part of the data gathered at MKWC and are operationally assimilated into LAPS along with synoptic observations, two soundings, and radiances from three *GOES-10* (IR, WV, and VIS) channels. An MM5 forecast initialized with LAPS analyses and an MM5 forecast initialized using the GFS analyses only as initial conditions are each run twice daily (at 0000 and 1200 UTC). The model performance as a function of the initial conditions used has been investigated through analysis of the model RMSE for select fields. A positive impact is found from data assimilation through LAPS. It is reasonable to attribute this positive result to the satellite data (both radiances and AMV) since they provide the greatest contribution to the LAPS analyses, given the relatively data sparse ocean surrounding Hawaii.

This study provides a simple evaluation of forecast improvement as a result of direct AMV and radiance data assimilation into mesoscale model initial conditions using LAPS. Future efforts will be directed toward implementation of a more complex assimilation system, such as three- and four-dimensional variational data assimilation analyses. However, these are computationally expensive and require additional resources. AMV data are now being provided with quality indicators (QI) for each observational datum, which is an independent measure of quality that can be used in the assimilation process (Holmlund et al. 2001). Sensitivity

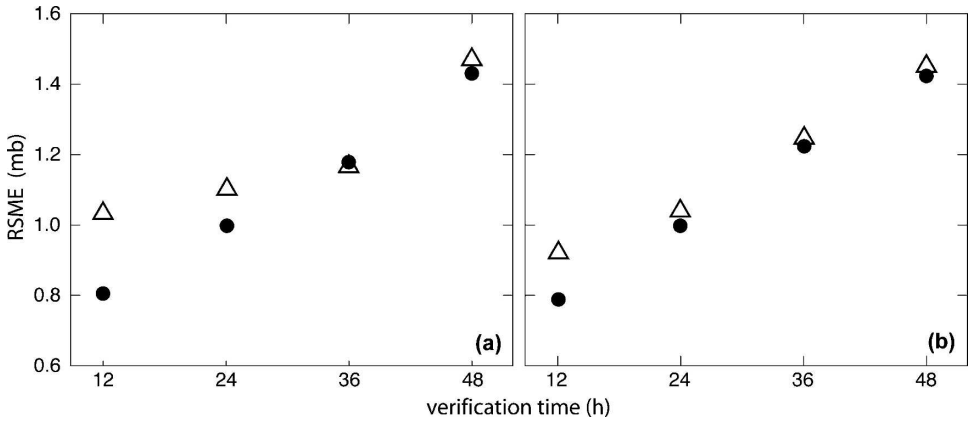

FIG. 9. Mean sea level pressure (mb) RMSE at four different verification times (t_0 + 12 h, t_0 + 24 h, t_0 + 36 h, t_0 + 48 h) averaged over all grid points and over the verification period (February–March). Dots represent RMSE values from MM5 forecasts initialized with LAPS analyses, and triangles are RMSE values from MM5 forecasts without LAPS. Results from runs initialized at (a) 0000 and (b) 1200 UTC, respectively.

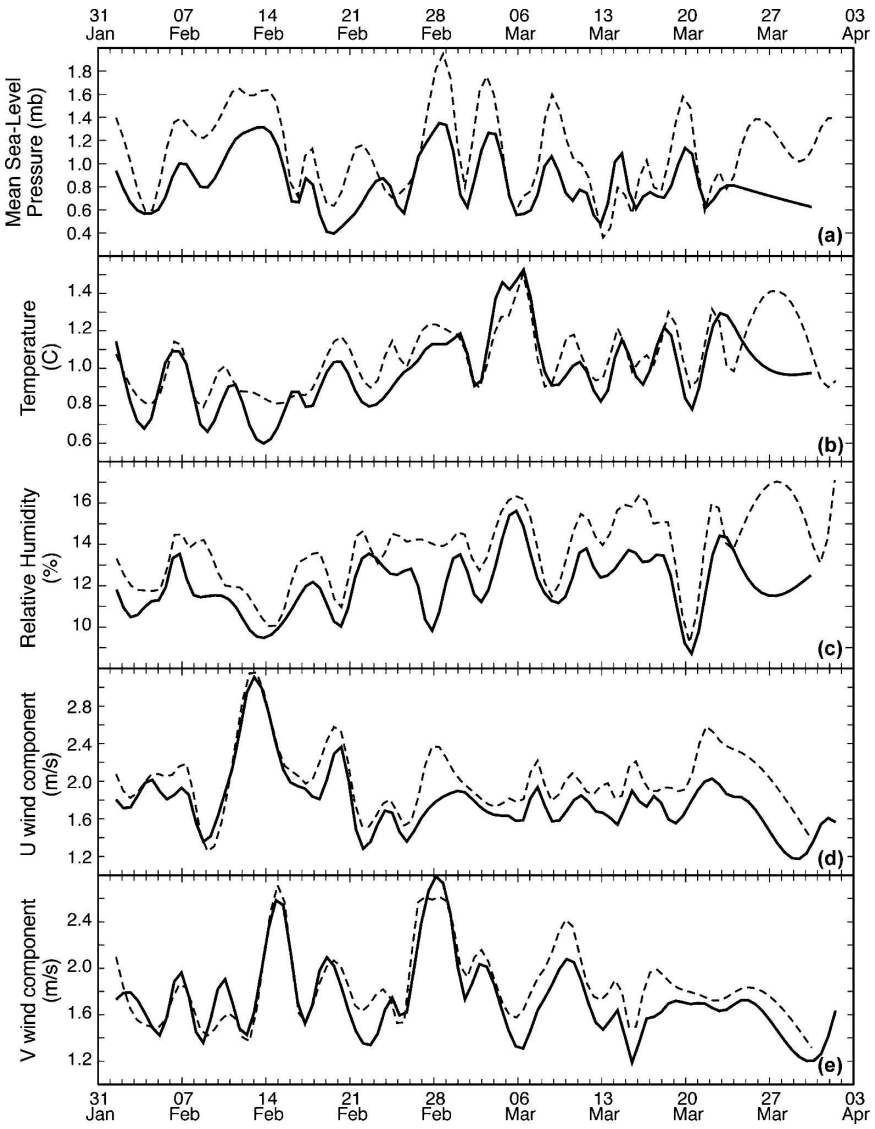

FIG. 10. Time series of RMSE for (a) mean sea level pressure (b) temperature, (c) relative humidity, and (d) u and (e) v wind components at 850 mb. The solid lines show 12-h forecast values from MM5 initialized with LAPS at 0000 UTC, and the dashed thin lines refer to 12-h forecast values from MM5 without LAPS at 0000 UTC.

simulations using the provided QI will be included in the future studies.

Acknowledgments. We thank Steven Albers, John McGinley, and John Smart at NOAA/Forecast Systems Laboratory for their help in implementing LAPS over the central Pacific. Nancy Hulbirt provided assistance with the graphics. The National Astronomical Observatory of Japan provided computer resources that are located at the Subaru Telescope facility in Hilo, Hawaii, for the MM5 simulations. The CIMSS research and development of automated AMV extraction methods from GOES are supported by the NOAA/NESDIS Office of Research and Applications. This research was supported by NOAA under Grant NA17EC1105.

REFERENCES

Albers, S., 1995: The LAPS wind analysis. *Wea. Forecasting,* **10,** 342–352.

Businger, S., and R. J. Reed, 1989: Cyclogenesis in cold air. *Wea. Forecasting,* **4,** 110–133.

——, R. McLaren, R. Okasawara, D. Simons, and R. J. Wainscoat, 2002: Starcasting. *Bull. Amer. Meteor. Soc.,* **83,** 858–871.

Cherubini, T., A. Ghelli, and F. Lalaurette, 2002: Verification of precipitation forecasts over the alpine region using a high-density observing network. *Wea. Forecasting,* **17,** 239–249.

Garand, L., 1983: Some improvements and complements to the infrared emissivity algorithm including a parameterization of the absorption in the continuum region. *J. Atmos. Sci.,* **40,** 230–244.

Grell, G. A., J. Dudhia, and D. R. Stauffer, 1995: A description of the fifth-generation Penn State/NCAR Mesoscale Model (MM/5). Tech. Note NCAR/TN-398+STR, National Center for Atmospheric Research, Boulder, CO, 122 pp.

Holmlund, K., C. Velden, and M. Rohn, 2001: Enhanced automated quality control applied to high-density satellite-derived winds. *Mon. Wea. Rev.,* **129,** 517–529.

Kain, J. S., and J. M. Fritsch, 1990: A one-dimensional entraining/detraining plume model and its application in convective parameterization. *J. Atmos. Sci.,* **47,** 2784–2802.

Klinker, E., F. Rabier, and R. Gelaro, 1998: Estimation of key analysis errors using the adjoint technique. *Quart. J. Roy. Meteor. Soc.,* **124,** 1909–1933.

McGinley, J. A., 1989: The Local Analysis and Prediction System. Preprints, *12th Conf. on Analysis and Forecasting,* Monterey, CA, Amer. Meteor. Soc., 15–20.

——, S. C. Albers, and P. A. Stamus, 1991: Validation of a convective index as defined by a real-time local analysis system. *Wea. Forecasting,* **6,** 337–356.

Morrison, I. J., and S. Businger, 2001: Synoptic structure and evolution of a kona low. *Wea. Forecasting,* **16,** 81–98.

Neiman, S., W. P. Menzel, C. M. Hayden, D. Gray, S. T. Wanzong, C. S. Velden, and J. Daniels, 1997: Fully automated cloud-drift winds in NESDIS operations. *Bull. Amer. Meteor. Soc.,* **78,** 1121–1133.

Reisner, J., R. J. Rasmussen, and R. T. Bruintjes, 1998: Explicit forecasting of supercooled liquid water in winter storms using the MM5 mesoscale model. *Quart. J. Roy. Meteor. Soc.,* **124B,** 1071–1107.

Stephens, G. L., 1978: Radiation profiles in extended water clouds. Part II: Parameterization schemes. *J. Atmos. Sci.,* **35,** 2123–2132.

Throen, I., and L. Mahrt, 1986: A simple model of the atmospheric boundary layer: Sensitivity to surface evaporation. *Bound.-Layer Meteor.,* **37,** 129–148.

Velden, C. S., C. M. Hayden, S. J. Nieman, W. P. Mensel, S. Wanzong, and J. S. Goerss, 1997: Upper-tropospheric winds derived from geostationary satellite water vapor observations. *Bull. Amer. Meteor. Soc.,* **78,** 173–195.

——, and Coauthors, 2005: Recent innovations in deriving tropospheric winds from meteorological satellites. *Bull. Amer. Meteor. Soc.,* **86,** 205–223.